

Experimental Demonstration of Relativistic Electron Cooling

Sergei Nagaitsev, Daniel Broemmelsiek, Alexey Burov, Kermit Carlson, Consolato Gattuso, Martin Hu, Thomas Kroc, Lionel Prost, Stanley Pruss, Mary Sutherland, Charles W. Schmidt, Alexander Shemyakin, Vitali Tupikov, and Arden Warner
FNAL, P.O. Box 500, Batavia, Illinois 60510, USA

Grigory Kazakevich
Budker INP, Novosibirsk 630090, Russian Federation

Sergey Seletskiy
University of Rochester, Rochester, New York 14627, USA
(Received 22 November 2005; published 30 January 2006)

We report on an experimental demonstration of electron cooling of high-energy antiprotons circulating in a storage ring. In our experiments, electron cooling, a well-established method at low energies (<500 MeV/nucleon), was carried out in a new region of beam parameters, requiring a multi-MeV dc electron beam and an unusual beam transport line. In this Letter, we present the results of the longitudinal cooling force measurements and compare them with theoretical predictions.

DOI: [10.1103/PhysRevLett.96.044801](https://doi.org/10.1103/PhysRevLett.96.044801)

PACS numbers: 29.27.Eg, 29.27.Fh, 29.20.Dh, 41.75.-i

Lack of radiation damping for heavy particles complicates their accumulation. The total six-dimensional phase-space density of antiproton beams, produced by striking dense targets with high-energy protons, cannot be increased by external fields independent of the particle motion [1]. In 1967, Budker described the method of “electron cooling,” a method of damping through the interaction between the antiproton (or proton) and an electron beam propagating together at the same average velocity [2]. He envisioned that “high-temperature” antiprotons, emerging from the production target, could be captured in a storage ring and their phase-space density could be increased through electron cooling. The accumulated antiprotons could then be used for colliding-beam or other experiments. The electron cooling method was successfully tested in 1974 at NAP-M (Russian acronym for Antiproton Accumulator Model) with low-energy nonrelativistic protons [3]. This method found a wide range of applications in several low-energy proton and ion storage rings [4], yet Budker’s vision of using electron cooling for relativistic antiprotons in collider experiments has never been realized, until now.

In 1995, Fermilab started a research and development program in relativistic-energy electron cooling in anticipation of increased antiproton production rates provided by improved stochastic cooling systems of the Fermilab antiproton source. The idea was not entirely new at that time; it had been proposed as an upgrade path for the Fermilab antiproton source as early as 1983 [5], and there had been some experimental work as well as conceptual development [6].

At Fermilab, antiprotons are produced by striking an inconel target with 120 GeV/ c protons. The 8.9 GeV/ c antiprotons are initially captured and cooled stochastically

in a storage ring, called the Accumulator. Fermilab has recently added another antiproton storage ring, the Recycler [7], to provide the final stages of cooling to the antiprotons prior to being transferred to the Tevatron collider. In 2004–2005, an electron cooling system was installed in one of the straight sections of the Recycler ring. In this Letter, we present the first electron cooling rate measurements for relativistic antiprotons in the Recycler storage ring.

Electron cooling of 8.9 GeV/ c antiprotons requires an electron beam with kinetic energy of 4.3 MeV. Figure 1 shows the schematic layout of the Recycler electron cooling system. Table I presents the basic parameters of the Recycler ring and its electron cooling system.

The dc electron beam is generated by a thermionic-cathode gun, located in the high-voltage (HV) terminal of the electrostatic (Van de Graaff-type) accelerator. This accelerator is incapable of sustaining dc beam currents to ground in excess of about 100 μ A. To attain the electron dc current of 500 mA, a recirculation scheme is employed. The electron beam is first delivered to the cooling section and then returned back to the HV terminal for charge recovery [8]. A typical inefficiency of such a process is 20 ppm for beam currents of up to 500 mA.

The electron cooling system at Fermilab employs a unique beam transport scheme [9]. The electron gun is immersed in a solenoidal magnetic field, which creates a beam with large angular momentum. After the beam is extracted from the magnetic field and accelerated to 4.3 MeV, it is transported to the 20 m long cooling section solenoid using conventional focusing elements. At the entrance to the cooling section solenoid, the beam is made round and parallel such that the beam radius r_b produces the same magnetic flux Br_b^2 as at the cathode.

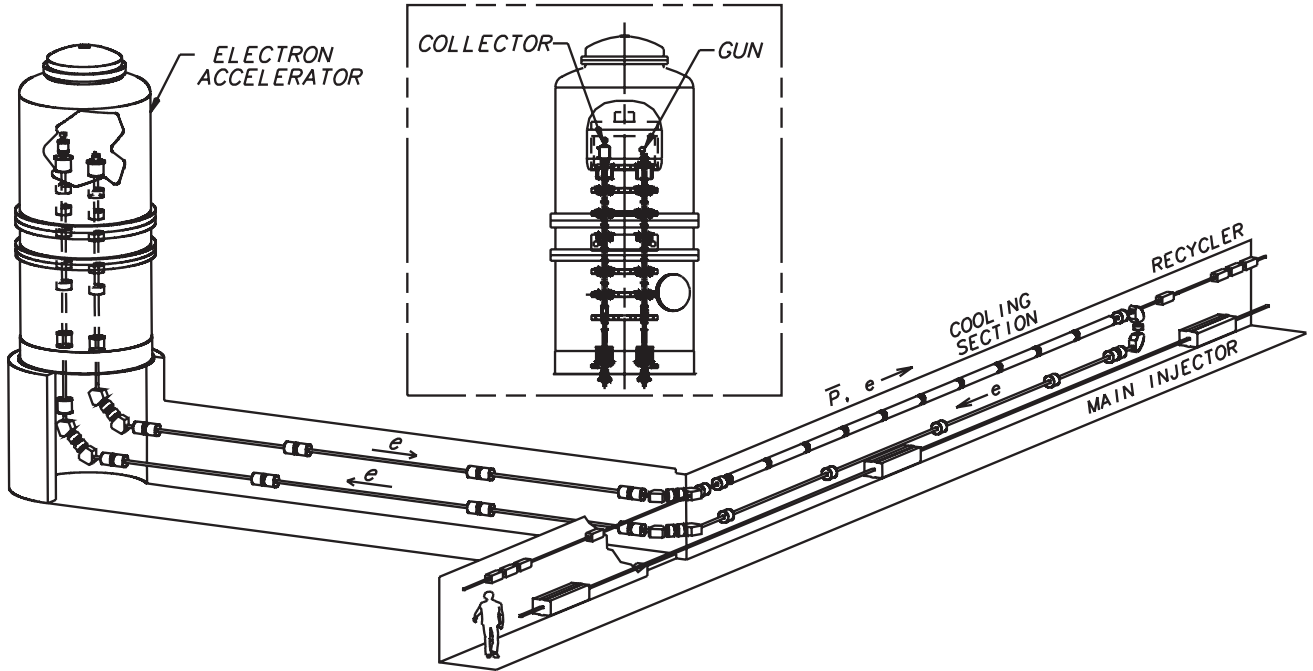


FIG. 1. Schematic layout of the Recycler electron cooling system and accelerator cross section (inset).

An antiproton traveling in an electron beam undergoes Coulomb scattering with electrons. The resulting friction force tends to bring such particles into thermal equilibrium with the electrons. Electron cooling can reduce the spread in all three components of beam momentum simultaneously. However, the Fermilab design is optimized for cooling primarily the longitudinal momentum spread.

Since the solenoid field in the cooling section is quite weak, the kinematics of the electron-antiproton scattering is weakly affected by the magnetic field. Unlike all existing electron coolers, our cooling system design employs non-magnetized cooling. In the electron beam rest frame (BF), an antiproton, moving through an electron gas with velocity \mathbf{v}_p , experiences a friction force [10]

$$\mathbf{F} = 4\pi n_e m (r_e c^2)^2 \Lambda \int_{-\infty}^{+\infty} f(\mathbf{v}_e) \frac{\mathbf{v}_e - \mathbf{v}_p}{|\mathbf{v}_e - \mathbf{v}_p|^3} d^3 \mathbf{v}_e, \quad (1)$$

where n_e is the electron density, m is the electron mass, r_e is the classical electron radius, c is the speed of light, Λ is the so-called Coulomb log (≈ 10 in our case), and $f(\mathbf{v}_e)$ is the electron velocity distribution function. As an illustration, let us assume that the electron BF velocities have an anisotropic Maxwellian distribution function

$$f(\mathbf{v}_e) = \frac{1}{(2\pi)^{3/2} \sigma_{\perp}^2 \sigma_{\parallel}} \exp\left[-\frac{v_{e\perp}^2}{2\sigma_{\perp}^2} - \frac{v_{e\parallel}^2}{2\sigma_{\parallel}^2}\right], \quad (2)$$

with σ_{\perp} and σ_{\parallel} being the transverse and longitudinal rms rest-frame velocity spreads. These two parameters can be expressed through laboratory-frame (LF) quantities in the following manner:

$$\sigma_{\perp} = \beta \gamma \theta_e c, \quad (3)$$

$$\sigma_{\parallel} \approx \frac{\delta E}{\beta \gamma m c}, \quad (4)$$

where δE is the LF rms energy spread of the electron beam. The electron energy spread, which in our case is approximately 300 eV, has three major components—(i) the power supply ripple δU , (ii) the multiple-

TABLE I. Electron cooling system and Recycler ring design parameters.

Parameter	Symbol	Value	Units
Electron accelerator			
Terminal voltage	U_0	4.34	MV
Beam current	I_b	0.5	A
Terminal voltage ripple, rms	δU	200	V
Cooling section			
Length	L	20	m
Solenoid field	B	100	G
Beam radius	r_b	3.5	mm
Electron angular spread, rms	θ_e	≤ 0.2	mrad
Recycler design parameters			
Circumference	C	3.3	km
Momentum	$\beta \gamma M c$	8.9	GeV/c
Transition γ	γ_t	20.8	
Average beta functions	β_{ave}	30	m
Typical emittance (n , 95%)	ε	5–7	$\mu\text{m rad}$
Number of antiprotons	N_a	≤ 600	10^{10}
Average pressure	P_{av}	0.5	nTorr

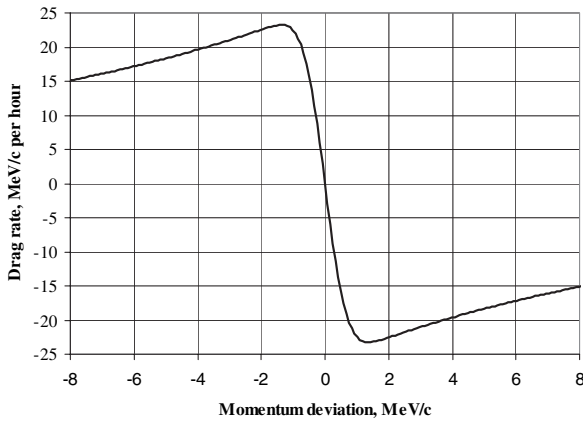


FIG. 2. The calculated longitudinal LF cooling force as a function of the antiproton energy deviation.

Coulomb scattering contribution, and (iii) the electron beam density fluctuations.

To express the cooling force equation (1) through LF quantities, one has to use proper Lorentz transformations and to recall that the cooling section occupies only a fraction of the ring circumference. It is convenient to represent the cooling force as a rate of LF momentum change for an antiproton of a given LF momentum deviation from its equilibrium value $\beta\gamma Mc$. Figure 2 presents the numerically calculated cooling force [Eq. (1)] for an antiproton with a zero transverse velocity as a function of its momentum deviation. The electron beam parameters were taken from Table I.

One can notice several features of the longitudinal cooling force in Fig. 2. First, the force is negative (positive) for positive (negative) momentum deviations. Second, for momentum deviations p smaller than ~ 1 MeV/ c , the force is a linear function of p

$$F_p \approx -\lambda p, \quad (5)$$

where λ is the so-called small-deviation cooling rate. For the cooling force shown in Fig. 2, the rate λ is ≈ 40 hr $^{-1}$. Finally, for larger momentum deviations the force decreases, though for the range of our interest (2 to 4 MeV/ c) only slightly. Below, we describe two techniques to measure the cooling force experimentally.

The first method allowed us to measure the small-deviation cooling force, Eq. (5). Initially, a very narrow (in momentum) antiproton beam distribution with a small transverse emittance was created by cooling the beam down to an equilibrium state. Figure 3 presents an example of such a distribution on a logarithmic scale. In equilibrium, the distribution function is Gaussian in momentum with an rms spread σ_0 being expressed as

$$\sigma_0 = \sqrt{\frac{D}{2\lambda}}, \quad (6)$$

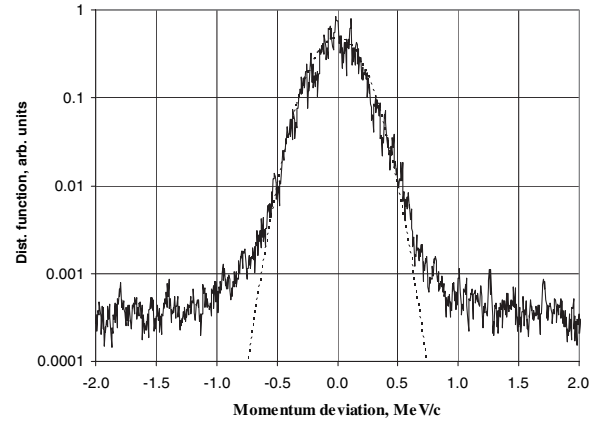


FIG. 3. Measured (solid curve) and Gaussian model (dashed curve) equilibrium distribution functions for a beam of 5×10^{10} antiprotons with the transverse emittance of $2 \mu\text{m rad}$ (n , 95%) cooled by a 500-mA electron beam. The rms momentum spread is 0.17 MeV/ c . Nonvanishing tails are due to amplifier noise.

where D is the diffusion rate, in our case mostly due to small-angle intrabeam scattering. The unknown diffusion rate D can be measured by turning the electron beam off and letting the beam heat up. Assuming that the diffusion rate D is constant, one can describe the rms momentum spread evolution with no cooling as

$$\sigma(t) = \sqrt{\sigma_0^2 + Dt}. \quad (7)$$

Figure 4 presents the measured evolution of the rms momentum spread after the electron beam was turned off temporarily and then on again. The best fit corresponds to $D \approx 2.5$ (MeV/ c) 2 /hr, which results in the cooling rate value being equal to $\lambda \approx 43$ hr $^{-1}$.

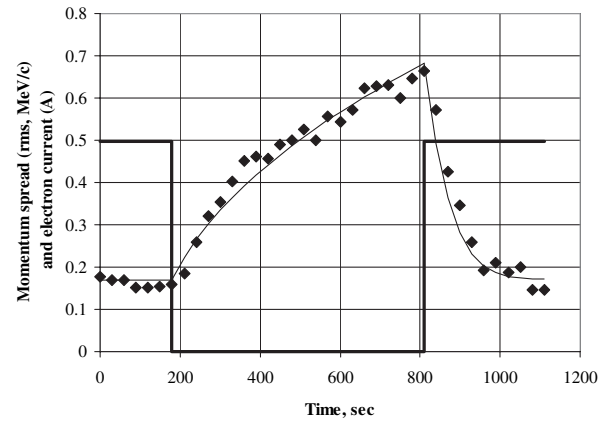


FIG. 4. The measured (diamonds) and the fitted (dashed line) rms momentum spread as a function of time. The electron beam current (solid line) was turned off at 180 seconds and on again at 810 seconds.

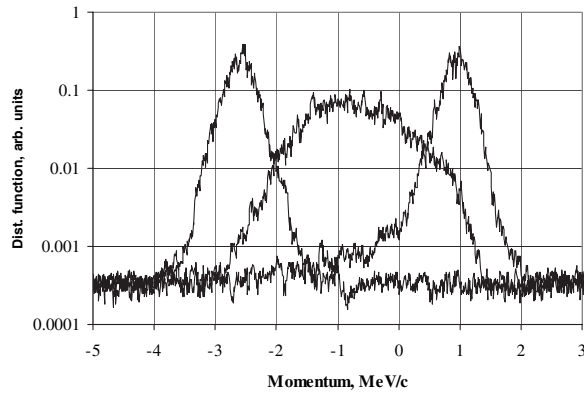


FIG. 5. The evolution of the antiproton beam momentum distribution function as the antiprotons are being dragged by the electron beam to a new equilibrium after the energy jump. Left curve, the initial distribution; center, 5 minutes later; and right, 17 minutes after the energy jump. The number of antiprotons was 4×10^{10} ; the transverse emittance was $1.6 \mu\text{m rad}$ (n , 95%).

With cooling, the rms momentum spread decreases as

$$\sigma(t) = \sqrt{\left(\sigma_1^2 - \frac{D}{2\lambda}\right) \exp(-2\lambda t) + \frac{D}{2\lambda}}, \quad (8)$$

which in Fig. 4 shows good agreement with the measured values.

The second technique applies to large-momentum deviations ($>2 \text{ MeV}/c$). The force can be measured by a voltage jump method [11]. In this method, the coasting antiproton beam is initially cooled down to a small equilibrium momentum spread. The electron beam energy is then changed instantaneously by several keV. The electron cooling force then drags the antiproton distribution to a new equilibrium momentum, which is M/m times the voltage jump away from the initial equilibrium. Figure 5 presents the evolution of the antiproton momentum distribution function as the antiprotons are being dragged by the electron beam after its energy was jumped by 2 keV.

The initial distribution (left curve, Fig. 5) as well as the final distribution (right curve, Fig. 5) are more narrow than the intermediate curve. We attribute it to the presence of diffusion and to the fact that the cooling force depends on the betatron amplitude of each antiproton within the distribution—particles with smaller amplitudes are cooled faster. We can characterize each distribution at a given time by its mean momentum. For the electron beam of 500 mA, the initial rate of change of the mean momentum for the 2 keV jump is $19 \text{ MeV}/c$ per hour. In Fig. 2, this value should be compared with the cooling force at $3.7 \text{ MeV}/c$, which is about $20 \text{ MeV}/c$ per hour.

Finally, Fig. 6 presents the momentum distribution function of a bunched 3×10^{12} antiproton beam stored in the Recycler with the help of electron cooling. To date, this is the largest number of antiprotons ever stored in a storage

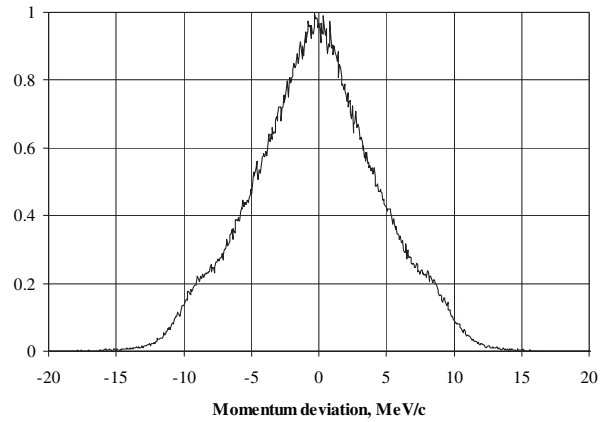


FIG. 6. The momentum distribution function (arbitrary linear scale) of 3×10^{12} bunched antiproton beam cooled by a 500-mA electron beam. The antiproton beam transverse emittance was $7 \mu\text{m rad}$ (n , 95%).

ring. Previously, with the stochastic cooling system alone, the Recycler was able to maintain about 1.8×10^{12} antiprotons in the same phase-space volume.

In conclusion, we have experimentally demonstrated electron cooling of relativistic $8.9 \text{ GeV}/c$ antiprotons and measured both small- and large-momentum deviation cooling force values. The measured cooling force is in agreement with theoretical predictions. The electron cooling system has been used in the Tevatron collider operations since August 2005. Since then, it has been primarily responsible for the recent advances in the Tevatron peak luminosity.

We thank D. Prasuhn, A.C. Crawford, T. Ellison, V. Lebedev, I.N. Meshkov, V.V. Parkhomchuk, and V. Reva for their help and fruitful discussions. Fermilab is operated by Universities Research Association Inc. under Contract No. DE-AC02-76CH03000 with the United States Department of Energy.

-
- [1] S. van der Meer, *Rev. Mod. Phys.* **57**, 689 (1985).
 - [2] G. I. Budker, *At. Energ.* **22**, 346 (1967) [*Sov. At. Energy* **22**, 438 (1967)].
 - [3] G. I. Budker *et al.*, *Part. Accel.* **7**, 197 (1976).
 - [4] I. N. Meshkov, *Phys. Part. Nucl.* **25**, 631 (1994).
 - [5] D. B. Cline *et al.*, *IEEE Trans. Nucl. Sci.* **30**, 2370 (1983).
 - [6] D. J. Larson, Ph.D. dissertation, University of Wisconsin, Madison, WI, 1986.
 - [7] G. Jackson, Fermilab Report No. FERMILAB-TM-1991, 1996.
 - [8] A. Shemyakin *et al.*, *Nucl. Instrum. Methods Phys. Res., Sect. A* **532**, 403 (2004).
 - [9] A. Burov *et al.*, *Phys. Rev. ST Accel. Beams* **3**, 094002 (2000).
 - [10] Ya. S. Derbenev and A. N. Skrinsky, *Part. Accel.* **8**, 1 (1977).
 - [11] H. Danared *et al.*, *Phys. Rev. Lett.* **72**, 3775 (1994).